

7 Fluidisation

The fluidisation principle is straightforward: passing a fluid upwards through a packed bed of solids produces a pressure drop due to fluid drag. When the fluid drag force is equal to the bed weight the particles no longer rest on each other; this is the point of fluidisation. The superficial velocity at this point is known as the 'minimum fluidising velocity' (U_{mf}). If the fluid velocity is increased further the pressure drop does not significantly increase – it remains equal to the bed weight per unit area, but the bed may expand; i.e. grow taller as illustrated in Figure 7.1. Commercial gaseous fluidised beds are usually operated at flow rates many times that required for minimum fluidisation, typically 5 to 20 times. Liquid fluidised beds operate at values closer to U_{mf} . A material balance indicates that, in general

$$C_i = \frac{C_f H_o}{H_i} \quad (7.1)$$

On page 53, the hypothetical case was made for turning the vessel containing hindered settling solids upside down and noting that the liquid velocity upwards, required to maintain the position of the interface, is equal to the settling velocity of the solids in an otherwise stationary liquid. This upward fluid flow, and balance of forces, is the hydrodynamic condition that exists during fluidisation. Thus, the Richardson and Zaki equation, page 54, is also valid for liquid fluidised systems and the minimum fluidising velocity is a superficial velocity, as illustrated in Figure 6.1 inverted.

Fluidisation is a popular means of contacting solids and a fluid because of the high degree of mixing and the resulting high transfer coefficients (heat and mass). There are numerous examples including: catalytic conversion of hydrocarbons, drying, combustion, calcination (application of heat to decompose a solid – for example calcium carbonate to oxide or gypsum solids to plaster), agglomeration, etc. Another useful advantage is the uniformity of the bed temperature, so that heat sensitive materials can be treated in a well controlled environment. However, the biggest disadvantage of gas beds is the need for dust control and treatment – which can be more expensive than the capital and running cost of the fluidised bed itself. An example of a gaseous fluidised bed is provided in Figure 7.2. In the figure several important aspects are recorded: the gas fluidised bed is not uniform, but bubbles of gas within the bed are observed (see Section 7.2), a distributor plate supports the solids and distributes the fluidising gas, above the bed the vessel diameter increases thereby reducing the gas velocity so that entrained particles may drop back into the bed from the *freeboard* and a gas cyclone is used for primary particle separation from the gas stream. The cyclone dip tube enters the bed – hence preventing gas from entering the cyclone from the

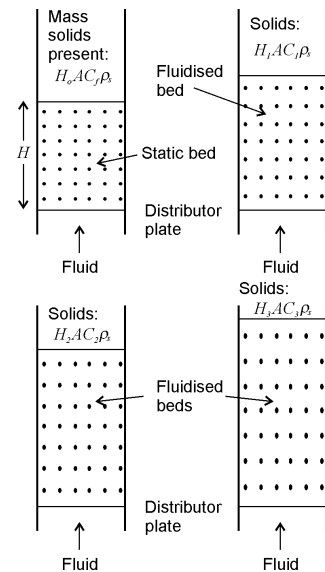


Fig. 7.1 Bed expansion during particulate fluidisation – mass of solids is the same in all beds

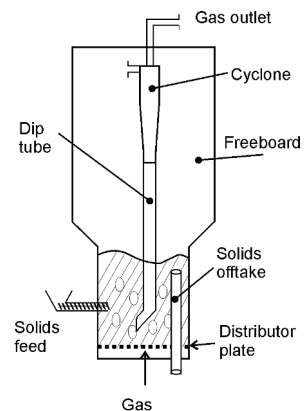


Fig. 7.2 Example design of a gas fluidised bed

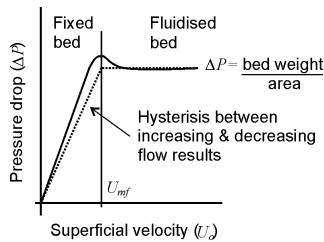


Fig. 7.3 Up to the fluidisation point pressure with superficial velocity is linear in accordance with Darcy's law:

$$\Delta P = \frac{\mu}{k} L U_o$$

On increasing the flow particles rearrange before fluidisation giving rise to the maximum - on decreasing flow a lower pressure drop may be found, giving a hysteresis.

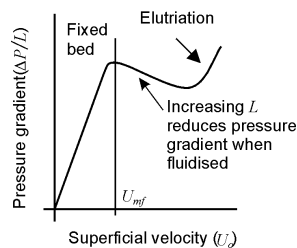


Fig. 7.4 Pressure gradient with superficial velocity up to and after fluidisation - linear as above whilst L is constant, but drops when L increases:

$$\frac{\Delta P}{L} = \frac{\mu}{k} U_o$$

solid's outlet. The cyclone inlet is simply open to the freeboard. Solids feed into a fluidised bed is often a significant challenge. Screw feeders used on free flowing materials may form a seal to prevent the gas escaping but, this cannot be guaranteed and rotary valves may need to be used. Reaction rates within the fluidised bed are usually rapid, hence the bed material is often inert, or reaction product, the actual amount of solid reacting within the bed may be very small; e.g. in fluidised bed combustion of coal a bed of calcium carbonate may be used and the coal particles may only be between 1/2 to 2% of the bed by mass. The calcium carbonate becomes oxide and then reacts to form calcium sulphate if sulphur dioxide is present. This provides in-situ sulphur dioxide emission removal. A high pressure drop over the distributor plate is usually required to ensure adequate distribution of fluidising gas over the entire area of the bed. Solids off-take can be by a simple overflow or via the gas outlet, or cyclone.

7.1 Minimum fluidising velocity

The fundamental equation for fluid flow through porous media, under laminar flow conditions, is Darcy's law, equation (3.4). In most instances the Kozeny-Carman equation (3.7) is preferred because it has an explicit expression for permeability in terms of bed porosity and specific surface. The pressure at the base of a fluid (due to fluid weight) comes from the static component of Bernoulli's equation

$$\Delta P = L \rho g$$

where L is fluid height, g is the acceleration due to gravity and ρ is the fluid density. For a suspension, a similar equation is valid but, for the *static pressure due to the solid particles*, we must take account of buoyancy and the proportion of particles present. Clearly, if there are no solids present there would be zero static pressure due to solids - but rather than use the solid concentration by volume fraction we use the porosity, see Figure 3.1, thus

$$\Delta P = L(\rho_s - \rho)g(1 - \varepsilon) \quad (7.2)$$

where ρ_s is the true solid density (kg m^{-3}). Combining equations (7.1) and (3.4) - remembering that we stated that fluidisation occurs when the bed weight (per unit area) equals the fluid drag gives

$$U_{mf} = \frac{k}{\mu} (\rho_s - \rho)g(1 - \varepsilon) \quad (7.3)$$

N.B. the minimum fluidising velocity is a superficial velocity (not interstitial). It is common to see equation (7.3) written with the permeability term expanded as provided by the Kozeny-Carman equation, see equation (3.7), and assuming spherical particles, equation (3.8), gives an alternative equation for minimum fluidising velocity

$$U_{mf} = \frac{(\rho_s - \rho)g \varepsilon^3 x_{sv}^2}{180(1 - \varepsilon)\mu} \quad (7.4)$$

7.2 Types of fluidisation

On increasing the fluid velocity, up to the point of fluidisation, flow patterns are usually well described by Darcy's law. However, after the fluidisation point two very distinct types of fluid flow are observed: *particulate* and *aggregative* fluidisation. In the former case the bed behaves in a uniform manner: as the flow rate is increased the bed height increases; hence, the increasing fluid flow simply goes to expand the bed, as illustrated in Figure 7.1. The overall pressure drop remains constant, and equal to the bed weight per unit area, until entrained particles are *elutriated* out by the fluid flow. In particulate fluidisation the fluid superficial velocity and bed porosity may be related by the Richardson and Zaki expression, see equation (6.1).

In aggregating, or bubbling, fluidisation aggregates (of fluid) may be observed within the fluidised bed that move rapidly to the surface. This type of fluidisation is often associated with the fluidisation of solids using gases. This is probably the most commercially important type of fluidisation. Hence, an understanding of aggregative, or bubbling, fluidisation is important. See the pictures of bubble formation and passage through a bed illustrated in Figure 7.5.

In an aggregative fluidised bed the fluid can pass through the bed in a similar fashion to particulate fluidisation *and* bubbles of fluid form. The bubbles may travel very quickly through the bed – hence in the case of catalytic cracking of hydrocarbons this provides a way in which some hydrocarbon vapour can by-pass the catalyst and, therefore, reaction. So, a bubbling bed has an *emulsion* phase surrounding the bubble and a *lean* phase where the bubble is lean of solids. These bubbles form spontaneously and, because most fluidisations of commercial interest take place in bubbling beds, a large amount of research has gone into characterising and understanding bubble behaviour.

There are several correlations designed to help answer the simple question: will a bed bubble or not? The simplest is based on the Froude number:

$$Fr = \frac{U_{mf}^2}{xg} \quad (7.5)$$

For high (>1) values bubbling is more likely. Other correlations include the use of Reynolds number, density ratio and bed ratio:

$$Re' = \frac{xU_{mf}\rho}{\mu}; \quad \frac{\rho_s - \rho}{\rho}; \quad \frac{L_{mf}}{d_b}$$

where L_{mf} is the bed height at minimum fluidisation and d_b is the bed diameter. The empirical correlations are:

$$Fr Re' \left(\frac{\rho_s - \rho}{\rho} \right) \left(\frac{L_{mf}}{d_b} \right) < 100 \quad \text{particulate fluidisation}$$

$$Fr Re' \left(\frac{\rho_s - \rho}{\rho} \right) \left(\frac{L_{mf}}{d_b} \right) > 100 \quad \text{bubbling fluidisation}$$

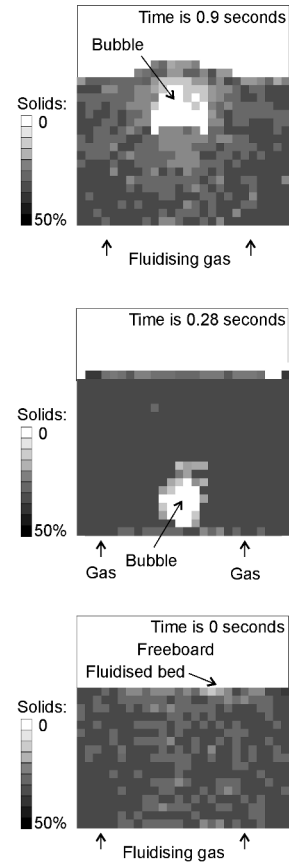


Fig. 7.5 Numerical simulation of aggregative (bubbling) fluidisation: a gas bubble rising in a fluidised bed. Note the scale bar on the left: white represents 100% voidage and black 50% voidage. The bed is just fluidised in the bottom picture.

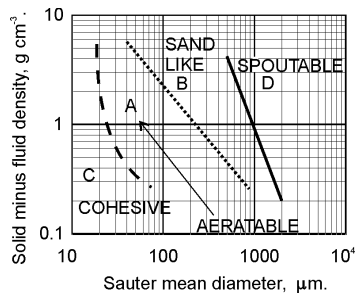


Fig. 7.6 Geldart's Powder Classification Chart for fluidisation

A more comprehensive attempt to describe fluidising behaviour, than the empirical correlations provided above, has been published and is known as the Geldart Powder Classification Chart (1973, *Powder Technology*, 7, p285), see Figure 7.6. The following regions are identified in Geldart's chart:

Group A: Aeratable, may not bubble, if it does then bed expands before bubbling, may have fast moving bubbles less than 100 mm.

Groups B & D: large bubbles, may form slugs. Group D gives slow bubbles.

Group C: Cohesive, high interparticle forces leads to difficult fluidisation, may form channels or slugs instead.

7.3 Bed design and bubbling behaviour

In practice, many different types of fluidisation may occur and the vessel geometry can influence this significantly. Figure 7.7 illustrates other fluidisation bed behaviour due to: slugging, channelling and spouting. In the latter two cases, a special design is sometimes used in which the bed is continually in axial motion, and a distributor plate might not be employed. Also included on Figure 7.7 is the effect of the bed behaviour on the pressure curve illustrated in Figure 7.3.

In another special case, the calcination of gypsum, a conical fluidised bed is used. The application here is to convert the gypsum (calcium sulphate dihydrate) into plaster (calcium sulphate hemihydrate), for use as plasterboard on walls, fillers, etc. and the particles are gypsum produced from flue gas desulphurisation (FGD) at large power stations. The calcinations can be written:



The particle Sauter mean diameter is 40 μm and the density is approximately 2.4 g cm^{-3} . The powder is well into Geldart's Group A - which should provide a reasonable quality fluidisation, but the FGD process is a wet one and although the particles are dewatered the product still has sufficient residual moisture for the wetting force to be very strong - causing particle cohesion. Hence, the particles can behave cohesively and do not fluidise easily. The actual, and unusual, fluidised bed design used is illustrated in Figure 7.8. It does not employ a distributor plate and uses the combustion products from natural gas and air, as well as the generated one and a half moles of water vapour per mole of calcium sulphate, as the fluidising media. Typical throughputs of 40 tonnes per hour for a fluidised bed 2.5 m in diameter are possible.

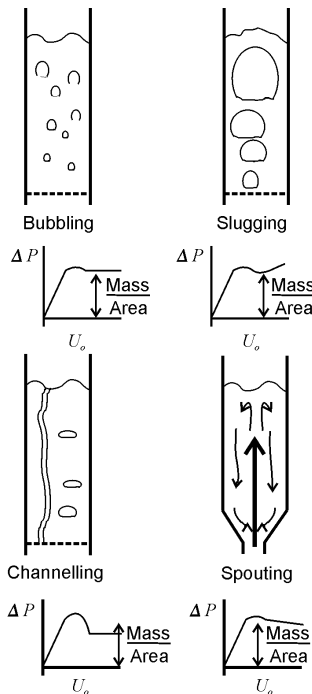


Fig. 7.7 Bubbling behaviour

7.4 Gas flow patterns around bubble and stability

A bubble is stable so long as particles that are drawn up into the bubble from underneath; i.e. are carried into the bubble by the fluid, can fall back out again. Unstable bubbles fill in with particles from the bottom. A simple schematic diagram of a gas bubble, within a surrounding emulsion phase of the fluidised bed, is illustrated in

Figure 7.9. Real bubbles tend to be more mushroom shaped than spherical but spheres are assumed for easier modelling. Two different gas flow patterns may be observed around a bubble; depending upon the speed of the bubble through the bed relative to the velocity of the gas through the surrounding emulsion phase. These two types are illustrated in Figure 7.10. When the gas bubble is travelling slower than the gas within the surrounding fluidised bed, the presence of the bubble will provide a region that has lower resistance to the gas flow than the surrounding emulsion phase. Hence, the gas will use the *path of least resistance* and there will be a tendency for gas to pass through the bubble in preference to the surrounding emulsion phase. Thus, lines representing the gas flow will bend towards the bubble and, after passing through the bubble, the lines will bend away from it again. This is similar to lines of electrical flux, or magnetism, bending towards a region of higher conductivity within an otherwise uniformly resistant matrix.

When the gas bubble travels faster than the gas in the surrounding fluidised bed, the gas that leaves the bubble at the top will then be immediately overtaken by the bubble (as it is travelling faster than the gas in the bed). Thus, the gas below the bubble will be the gas that recently left it at its top and will re-enter the bubble. The gas flow pattern is one in which gas recirculates around a fast moving bubble. The gas does come into contact with some of the solids within the bed, but only those within the *cloud* associated with the bubble. Hence, the speed of the bubbles through the bed and the restricted contact of gas with solid particles means that this type of fluidisation can have poorer fluid-solid contacting than the slower moving bubbles and particulate fluidisation. One of the first successful mathematical analyses of this type of fluidisation was by Davidson and Harrison, in the 1960's.

7.5 Davidson and Harrison model

The model assumed that the fluidised particles can be treated as an incompressible fluid, called the particulate phase, which has the same porosity as the bed when it just became fluidised, i.e. at *incipient fluidisation*. The model also assumed that the fluid can occupy the same space as the particulate phase and can be treated incompressibly, and that the fluid and particulate phases can be linked by Darcy's law. The model is based on gas velocities centred around a bubble; hence spherical polar coordinates were used, this is illustrated in Figure 7.11 and U_θ and U_r represent the gas angular velocity in the plane of the paper and towards (and away from) the centre of the circle. The resulting model gives the gas velocities as

$$U_r = \left[\frac{R_b^3}{r^3} (U_b + 2U) - (U_b - U) \right] \cos \theta \tag{7.6}$$

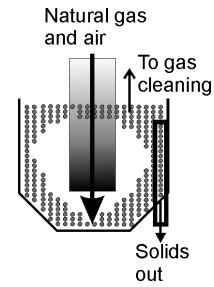


Fig. 7.8 Conical kettle type fluidised bed – no distributor plate

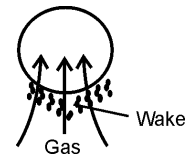


Fig. 7.9 Gas bubble with solids trapped in wake

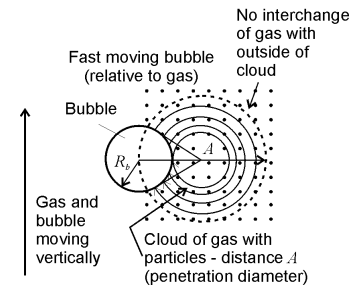
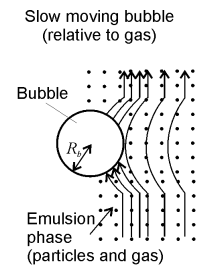


Fig. 7.10 Slow and fast moving bubbles

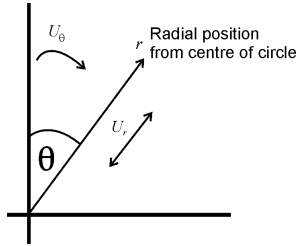


Fig. 7.11 Illustration of spherical polar coordinates

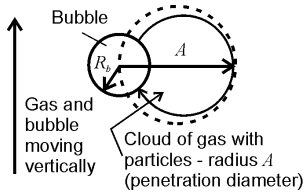


Fig. 7.12 Fast moving bubble and cloud

$$U_{\theta} = \left[\frac{R_b^3}{r^3} (U_b / 2 + U) + (U_b - U) \right] \sin \theta \quad (7.7)$$

where U is the interstitial gas velocity, U_b is the bubble velocity, R_b is the radius of the bubble and r is the radial coordinate (i.e. distance from bubble centre). The gas velocity in the azimuthal direction is assumed to be zero; i.e. the angular velocity of the gas coming out of the plane of the paper is zero.

Considering Figure 7.12 representing a fast moving bubble, on the horizontal plane the gas flow rate upwards though the bubble will be the same as that going downwards through the cloud because there is no interchange of gas with the surroundings. Hence, using A for the cloud radius, the gas flow rate through the bubble will be equal to

$$\int_{R_b}^A 2\pi r \varepsilon U_{\theta} dr \quad (7.8)$$

At an angle of 90° $\sin\theta$ is unity, hence the gas flow rate will be

$$\int_{R_b}^A 2\pi \varepsilon r \left[\frac{R_b^3}{r^3} (U_b / 2 + U) + (U_b - U) \right] dr \quad \text{which integrates to give}$$

$$\pi \varepsilon \left[(U_b + 2U) R_b^3 \left(\frac{1}{R_b} - \frac{1}{A} \right) + (U_b - U) (A^2 - R_b^2) \right] \quad (7.9)$$

Now considering the periphery of the cloud, where there is no interchange of gas with the surroundings, $U_r \rightarrow 0$ and $r=A$ can be used in equation (7.6) to provide

$$\frac{R_b^3}{A^3} = \frac{(U_b - U)}{(U_b + 2U)} \quad (7.10)$$

with rearrangement and substitution into equation (7.9)

$$\text{gas flow rate} = -2\pi \varepsilon (U_b - U) \left(1 - \frac{A^3}{R_b^3} \right) \frac{R_b^2}{2} \quad (7.11)$$

Equation (7.10) can be used to relate cloud and bubble radii, thus

$$\text{gas flow rate} = -\pi \varepsilon R_b^2 (-U_b - 2U) = 3\pi \varepsilon R_b^2 U \quad (7.12)$$

Using the assumption that the gas in the emulsion phase has the same velocity as it did at incipient fluidisation, then the interstitial velocity will be

$$U = U_{mf} / \varepsilon_{mf} \quad (7.13)$$

and the porosity of the emulsion phase remains substantially unaltered from that of ε_{mf} thus combining equations (7.12) and (7.13)

$$\text{gas flow rate} = 3\pi R_b^2 U_{mf} \quad (7.14)$$

Equation (7.14) suggests that the gas flow rate going through a bubble is three times the minimum fluidising velocity flowing over the bubble cross-sectional area. Another significant result from the concepts used in this modelling is that the gas in excess of that

Crossover velocity

At $U=U_b$ gas recirculation in the cloud extends over:
 $A \rightarrow \infty$

i.e. crossover between the two types of flow round a bubble shown in Figure 7.10. So, at crossover:

$$U_b = \frac{U_{mf}}{\varepsilon_{mf}}$$

and U_{mf} may come from equation (7.4). This links the properties of the particles, bubble size and fluidisation bubbling type.

needed to fluidise the bed will pass through the bed in bubbles. Hence, in aggregative fluidisation bed expansion will occur because of displacement of particulate phase bed by the bubbles, not due to the homogenous redistribution of solids represented by equation (6.1); i.e. the Richardson and Zaki equation is not valid for aggregative fluidisation.

The Davidson and Harrison model has been refined by other research workers since the 1960's, but it represents the starting point for many of these later models. Its advantages include: a relatively simple model to apply, appears to predict gas flow near a bubble, shows how gas can by-pass solids in a fluidised bed, explains stability of a bubble (by predicting gas flowing up through one) and it predicts pressure variation near a bubble reasonably. However, there are several deficiencies including: the bubble shape is wrong (mushroom shape is observed), it doesn't explain what happens when particles enter a bubble, the maximum predicted bubble size is wrong, it assumes incompressible phases and it uses Darcy's law to link the phases together. More recently, with the advent of increasing and readily available computing power an alternative approach to the analysis of homogeneous phases has been to consider the behaviour of individual particles themselves. This is known as Discrete Element Analysis, or Distinct Element Method.

7.6 Discrete element analysis

Discrete Element (DE) analysis has been applied to many different operations in particle technology, including: flow in hoppers, mixing, pneumatic conveying, etc. It is based on determining all the forces acting on a particle and computing the net acceleration to apply over a time increment. At the next time increment the step is repeated. Clearly, this is computationally very complex and it is usually applied to two dimensional simulations. However, the results can be more realistic than a continuum based modelling approach as described in the previous section. An example of the level of detail in results that is possible is given in Figure 7.5, which is based on a DE analysis conducted at Tsuji Laboratory, Osaka University.

In fluidisation, it is possible to model the particle movement by DE and a conventional numerical solution for the gas flow. Mass and momentum balances are applied within the solution. The particle motion is described by Newton's equation of motion, which in the context of the appropriate forces for fluidisation modelling can be stated as

$$\frac{d^2z}{dt^2} = (F_C + F_D + F_W) / m_p \quad (7.15)$$

where m_p is the particle mass and the forces are due to respectively: collision, fluid drag and gravity. Hence, under appropriate conditions equation (7.15) is solved to give

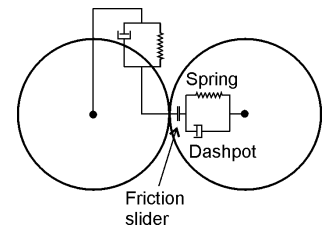


Fig. 7.13 Contact force between two particles represented by spring and dashpot

$$\frac{dz}{dt}_{t+\Delta t} = \frac{dz}{dt}_t + \frac{d^2z}{dt^2} \Delta t \quad (7.16)$$

and

$$z_{t+\Delta t} = z_t + \left(\left. \frac{dz}{dt} \right|_t + \left. \frac{dz}{dt} \right|_{t+\Delta t} \right) 0.5 \Delta t \quad (7.17)$$

The drag force used in the analysis usually comes from either the correlations described in Chapter 3, for the dense phase – such as Ergun’s correlation, or the drag coefficient described in Chapter 5, for a region dilute in particles.

The contact force consists of normal and tangential forces, which can be modelled in terms of a spring, dashpot and a friction slider as shown in Figure 7.13. The normal and tangential component of forces are expressed as the sum of the forces due to the springs and dash pots. The stiffness of the springs and the viscous dissipation coefficient of the dash pot determine the force with which the particles interact. A very soft spring would cause the particles to embed into each other, causing a large overlapping region between the particles. By allowing some particle overlapping in space it is possible to overcome the problem of defining how the particles deform on contact and the mathematical solution is simpler. In the model, two particles move towards each other until the contact force changes its sign; i.e. from attraction to repulsion. Contact between a particle and a wall is modelled in a similar way, except that the wall is stationary.

Modelling particle interaction with its neighbours and the wall is very computationally intensive and is restricted to simulations using several thousand particles, at best. This may be sufficient for a reasonable indication of the physics of what is taking place, but actual processes normally contain many millions of particles. Nevertheless, DE modelling of processes within particle technology will become more reliable and extensively used as computing power increases. They also have the advantage that additional forces can be added into the solutions, e.g. colloidal interaction, and that a range of particle sizes can be considered.

Specific surface

For gas phase reaction modelling the specific surface is often much greater than that provided by equations covered in Chapter 2. This is due to internal cracks and pores in catalyst particles. This area may be determined by gas phase adsorption tests. However, for calculations of pressure drop, e.g. equation (7.4), the particle envelope specific surface should be used. This is the same value as that covered in Chapter 2.

7.7 Summary

In a packed bed of static solids the weight of the particles is transmitted to the base by a network of contacts between the particles. The two forces present are the solids stress gradient (upthrust reaction force) and the particle weight. During upflow of fluid through the bed the equations for flow and drag, Darcy’s law or Carman correlation, are valid and at some point the fluid drag will equal the bed weight. This is the fluidising point. After the point of fluidisation the bed may expand further, the gaps between particles getting bigger. During fluidisation, the pressure loss of the fluid is equal to the bed weight and this will remain constant irrespective of the bed expansion. Hence, the pressure drop remains constant.

When fluidised, the bed adopts all the properties of a usual fluid including: lighter objects float, surface stays horizontal, solids would pour out of a hole in the vessel side, the level of two connected beds would be equal (like a U tube) and the *static* pressure within the bed is given by depth \times density. These properties assist in some of the advantages of a fluidised bed, which include: easy to control and automate, rapid mixing (excellent temperature control), large and small beds are usable, very high heat and mass transfer coefficients. Some of the disadvantages include: little scope for temperature gradients giving thermal shock, a good distributor plate is usually needed, expensive dust cleaning equipment may be necessary, particle breakup, erosion and stirred tank behaviour gives non-uniform residence times.

Fluidised beds are frequently used for reactors, such as the vapour phase catalytic cracking of hydrocarbons. In this operation multiple beds are used; cracking taking place in one bed under one set of reaction conditions and regeneration of catalyst in a separate bed. Transfer of catalyst is easily performed because of the fluidised behaviour of the solids being similar to that of a fluid. In liquid fluidisation, segregation between particles based on size and density difference is possible and this is used in the regeneration of bed filters using mixed beds of sand and carbon. Segregation is not so common in gas fluidised beds because solid/solid mixing is encouraged by entrainment of particles within the wake of the gas bubbles.

7.8 Problems

1. Minimum fluidising velocity (U_{mf}) is a superficial velocity. Use the Basic equations box to derive an equation for the minimum fluidising velocity where $U_{mf} = f[g, \rho_s, \rho, \mu, \varepsilon$ and diameter (x)]:

$$U_{mf} =$$

2.

i). A packed bed consisting of 1.96 kg of solids of density 2.8 g cm^{-3} is contained in a cylindrical vessel of 10 cm internal diameter, and the bed height is 20 cm. The volume of the vessel occupied by the bed is (ml):

a: 157 b: 1570 c: 3140 d: 6280

ii). The volume of the solids in the vessel is (ml):

a: 700 b: 1430 c: 70 d: 5490

iii). The porosity of the bed is (-):

a: 0.554 b: 0.773 c: 0.446 d: 0.227

iv). The particle size is $500 \mu\text{m}$ and the liquid density and viscosity are 1000 kg m^{-3} and 0.001 Pa s , minimum fluidising velocity is (m s^{-1}):

a: 9.4×10^{-6} b: 0.021 c: 0.017 d: 0.0094

v). Was the use of the Kozeny-Carman equation justified?

vi). What type of fluidisation is likely to occur?

Basic equations

The Kozeny-Carman equation for fluid flow through porous media is

$$\frac{\Delta P}{L} = \mu \left[\frac{5(1-\varepsilon)^2 S_v^2}{\varepsilon^3} \right] U_o$$

where ΔP is the pressure drop over the bed, L is the bed depth, μ is the viscosity, ε is the bed porosity, S_v is the specific surface area per unit volume of the particles and U_o is the fluid superficial velocity.

During fluidisation the pressure drop over a fluidised bed is constant and equal to the bed weight, i.e.

$$\Delta P = (1-\varepsilon)g(\rho_s - \rho)L$$

where g is the acceleration due to gravity and ρ and ρ_s are the fluid and solid densities respectively.

The *modified* Reynolds number (Re_1) is:

$$Re_1 = \frac{\rho U_o}{S_v(1-\varepsilon)\mu}$$

The Froude number (Fr) is:

$$Fr = \frac{U_{mf}^2}{gx}$$

Richardson and Zaki

$$U_o = U_t \varepsilon^n$$

where U_t is the terminal settling velocity (modified for wall effects if necessary) and n is an exponent defined as follows

$$n = 4.6 \quad ; \text{ at } Re' < 0.2$$

$$n = 4.4 Re'^{-0.03} \quad ; \text{ at } 0.2 < Re' < 1$$

$$n = 4.4 Re'^{-0.1} \quad ; \text{ at } 1 < Re' < 500$$

$$n = 2.4 \quad ; \text{ at } Re' > 500$$

3.

i). Another fluidised bed contains 1.8 kg of solids of density 1.3 g cm^{-3} in a cylindrical 30 cm internal diameter vessel, with a bed height of 20 cm. The bed porosity is (-):

a: 0.853 b: 0.976 c: 0.098 d: 0.902

ii). The particles used above have a diameter of $200 \mu\text{m}$ and the fluid density and viscosity are 1.29 kg m^{-3} and $2 \times 10^{-5} \text{ Pa s}$, respectively.

The terminal settling velocity of a particle is 0.783 m s^{-1} (from the Heywood Tables - check this), the *Particle* Reynolds number is, see Chapter 5:

a: 0.101 b: 10.1 c: 10200 d: 1×10^7

iii). For this system, the value of the exponent n in the Richardson and Zaki equation should be:

a: 3.49 b: 4.60 c: 4.11 d: 2.40

iv). The superficial velocity required to fluidise these particles to achieve the above conditions is (m s^{-1}):

a: 1.8×10^{-5} b: 0.71 c: 0.53 d: 0.55

v). The gas flow rate required to fluidise these particles to achieve the above conditions is ($\text{m}^3 \text{ s}^{-1}$):

a: 0.15 b: 380 c: 0.039 d: 3.9

4.

Estimate the bed expansion and bypass fraction for a fluidised bed with incipient fluidisation velocity of 0.1 m s^{-1} if it is operated at a superficial velocity of 0.15 m s^{-1} and has 2 cm diameter bubbles rising at 0.5 m s^{-1} . At incipient fluidisation the porosity is 0.4.

5.

A gas bubble in a fluidised bed reactor was found to be typically 100 mm in diameter and to be rising with a velocity of 0.5 m s^{-1} . Using the Davidson and Harrison model, investigate the particle size at which the transition in the gas flow pattern occurs: from bubbles rising slower than the interstitial gas velocity to bubbles with gas circulation between the bubble and its cloud. Assume typical values of particle physical properties; take the viscosity of air to be $2 \times 10^{-5} \text{ Pa s}$. Finally, draw an estimated graph of the thickness of the cloud surrounding a bubble of 100 mm diameter as a function of the size of the fluidised particles.

6.

Using the Davidson and Harrison two phase model, derive an equation for the rate of flow of gas into and out of a gas bubble in terms of bubble radius, interstitial velocity and bubble velocity. Discuss how the model may help in the design of catalytic fluidised bed reactors.

Hint Q.4

See comments at the foot of page 72. A volume balance is needed for the bed expansion.

Hint Q.5

See the box on crossover velocity on page 72.